

## Hydrologic Modeling System HEC-HMS Application for Direct Runoff Determination

Martheana Kencanawati <sup>1, 2\*</sup>, Data Iranata <sup>1</sup>, Mahendra A. Maulana <sup>1</sup>

<sup>1</sup> Department of Civil Engineering, Institut Teknologi Sepuluh Nopember, Keputih Sukolilo, Surabaya East Java 60111, Indonesia.

<sup>2</sup> Department of Civil Engineering, Balikpapan University, Damai Bahagia South Balikpapan, Balikpapan East Kalimantan 76114, Indonesia.

Received 03 March 2023; Revised 12 May 2023; Accepted 19 May 2023; Published 01 June 2023

### Abstract

The process of identifying the peak discharge using the rational method was introduced in the 1880s. This method is a simple procedure for determining the peak discharge derived from surface runoff flow. Therefore, this research modified a simple hydrological formulation (rational method) based on fieldwork and compared a numerical rainfall model to the relationship model by using the simulation parameters, namely rainfall, infiltration, land use, and stream for hydrological conditions. The novelty of this research is a modification of the theoretical formula (rational method) through the use of fieldwork factors to modify the run-off coefficient. The first scene-up was overlay mapping between land and land use shape files, while the scene-up sampling point was upstream and downstream. This was continued with the estimation curve number until a specific composite curve number was initiated. The rate of infiltration was determined using the Horton method to distinguish the soil type, while the Water Stage Data Logger Starter Kit 13" HOBO KIT-S-U20-04 was used to measure the water level, HEC HMS, and rating curve analysis. The relationships between the fieldwork data using hydrology analysis and modeling were then compared. The results showed that the maximum rainfall calculated and analyzed from the box-and-whisker plot was 140 mm in the year 2019. In addition, the infiltration rate at the upstream and downstream areas was 90 mm/hour and 26.4 mm/hour, or 30% out of the upstream area value. Finally, the estimations of the runoff coefficient were 0.60, 0.45, and 0.0133, while the discharges for the maximum rainfall intensity were observed at 405.7 m<sup>3</sup>/s, 304.3 m<sup>3</sup>/s, and 25 m<sup>3</sup>/s. The simulation using Hydrological Modelling HEC HMS 4.11 computed results of 0.1 m<sup>3</sup>/s and observed flow of 0.3 m<sup>3</sup>/s.

**Keywords:** Peak Flow; Runoff, Fieldwork; Infiltration; Curve Number; HEC-HMS 4.11.

### 1. Introduction

Excessive rainfall is the primary cause of flooding, as it results in runoff that cannot be absorbed into the soil surface or ground [1]. The following factors, including soil texture, moisture levels, compaction, land cover (including vegetation), and rainfall intensity, are known to influence both runoff and its associated coefficient [2]. Previous research stated that the value of the runoff coefficient depends on soil characteristics, land use, and topography [3]. In addition, numerical methods used for simulating rain flow often rely on rainfall, infiltration, land use, and flow parameter data to establish rainfall-runoff relationship models [4]. The rational method, influenced by factors such as rainfall intensity, infiltration rate, and the characteristics of ungauged catchments, plays a significant role in determining runoff flow [5]. However, both the rational and NRCS methods have the capacity to estimate the depth of surface runoff in each micro sub-basin [6].

\* Corresponding author: [martheana@uniba-bpn.ac.id](mailto:martheana@uniba-bpn.ac.id)

 <http://dx.doi.org/10.28991/HEF-2023-04-02-02>

➤ This is an open access article under the CC-BY license (<https://creativecommons.org/licenses/by/4.0/>).

© Authors retain all copyrights.

The NRCS-CN method is an empirical model designed to estimate the Q peak flow in ungauged catchments [7]. Impervious regions within a catchment area can also affect the determination of runoff discharge [8]. The rational method defines the ratio between inflow and outflow during a specific rain duration compared to the watershed time concentration ( $T_c$ ) [9]. The characteristics of a catchment area are closely associated with the runoff volume it experiences [10]. Simplified rational methods are capable of calculating peak flow in watersheds [11]. Peak flow is influenced by various factors, including the spatial distribution of temporal rainfall intensity, time of concentration ( $T_c$ ), and the curve number (CN), all of which contribute to catchment characteristics [12]. The time of concentration signifies the point at which water reaches the catchment outlet [13]. The modified rational method, as derived from NRCS models, can be used to estimate surface runoff depth in any sub-catchment [14]. The runoff coefficient (C) is the principle parameter in this method, and there exist various ways it could be estimated [15].

Hydrological models require the adjustment of parameter values to match specific watershed characteristics, a process achieved through the calibration and validation of observed river flows. Predicting river flow in ungauged catchment areas, where discharge data is lacking, poses a significant challenge in hydrology [16]. Sensitivity analysis (SA) plays a significant role in hydrological modeling, as it identifies parameters that exert a substantial influence on the model and those that have minimal impact. It offers valuable insights into the complex relationships among various model processes within the system [17]. The validity of the curve number model was established by ensuring the field observations made were in line with the functional forms of rainfall-runoff relationships [18]. This research examined an optimization scenario comprising two parameters with distinct variations [19]. The proposed hypothesis states that while the fundamental principles of hydrology are conceptually simple, their practical application demands a nuanced understanding, given the complexity of fitting theoretical hydrological formulas to real-life conditions [20]. The key parameters include precipitation, infiltration rate, soil type, land use and land cover, curve number, initial abstraction, and maximum storage capacity. The expected contribution of this research lies in its applicability in smaller catchment areas with incomplete data. It also aims to facilitate the application of rational methods, allowing for the estimation of C numbers within defined coefficient ranges. These estimates can then be used in ungauged catchments characterized by typical rainfall patterns as well as land use and land cover. This choice was driven by the fact that the basin area under investigation, approximately 91.526 km<sup>2</sup>, falls below the standard 100 km<sup>2</sup> required for applying other methods such as Weduwen or Hasper.

## 2. Method

In this research, the modified rational method was adopted to determine peak flow and calculate the runoff coefficient. This approach involved the integration of various techniques and tools, including observations, sampling, GIS mapping, sub-basin delineation, and the analysis of land use, soil type, and topography. Several significant parameters were utilized, including infiltration rate, curve number, Hydrologic Soil Group (HSG) classification for soil type, maximum storage capacity, initial abstraction, and time lag for modeling. The research process began with a GIS mapping overlay, followed by fieldwork conducted in the Lanang River catchment area. During this fieldwork, daily rainfall measurements were collected with the Wireless Weather Station Professional MISOL Wind Rain Humidity Gauge, using an automatic water level recorder and a double-ring infiltrometer. The flowchart in Figure 1 illustrates the various stages of research implementation, ultimately leading to the final scenario aimed at achieving the expected results.

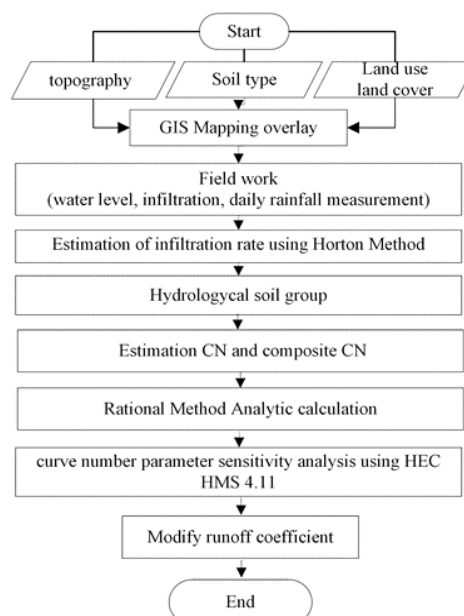


Figure 1. Study workflow

A series of measurements was conducted to determine the infiltration rate, with a double-ring infiltrometer employed to observe and record how water infiltrated the soil surface. Subsequently, the Horton equation was used to analyze the collected data. To monitor water levels in the Lanang River catchment area, automatic loggers were used. These loggers recorded water levels at hourly intervals from April 27 to October 10, 2022. Throughout this period, a dataset of 1526 water level measurements were accumulated, from April 27th to June 27th, 2022, and these were paired for simulations in HEC HMS 4.10. For collecting water level data, the HOBO KIT-S-U20-04 Water Level Data Logger Starter Kit (13") was used. These automatic water level loggers accurately combined the water level measurements with pressure data, as shown in Figures 2 and 3.



**Figure 2. Water Level Data Logger Starter Kit 13" HOBO KIT-S-U20-04 (Before installation inside the Lanang River)**



**Figure 3. Water level data logger starter kit 13" HOBO KIT-S-U20-04 Installation and Steel Pipe as a vessel of the HOBO KIT**

In the time series modeling scenario, fieldwork data comprising various aspects, including parameters and factors contributing to runoff generation, were systematically compared. The primary goal of this process was to transform these data points into models predicting peak flow and direct runoff within a specific catchment area. HEC HMS 4.10 offered two primary options for this transformation process, namely the empirical and conceptual/kinematic wave models, grounded in system theory and designed for overland flow, respectively. Within the HEC-1 model, an interconnected system of hydrological and hydraulic components designed to suit the basin was created, allowing for the simulation of surface runoff in rivers and watersheds. In addition, this comprehensive model considered rainfall data as well. Each component of the model relied on specific parameters with unique characteristics, and mathematical relationships were established to describe the physical processes.

The outcome of the modeling process was the generation of computational streamflow hydrographs that closely matched the observed conditions in the desired river basin location. To facilitate simulation modeling, HEC-1 divided the basin into sub-basins and reaches. This approach, known as the lumped-parameter model (ENVI 512, February 2003), necessitates the use of average values that represent the entire area or length of the stream for mathematical coefficients applied in hydrological and hydraulic computations. Throughout the process, HEC-HMS 4.10 served as a guide through the stages of calibration and simulation, comprising distribution and constant models, as well as interfaces with GIS data, including sub-basin and reaches shape files, to enhance the accuracy and relevance of the modeling efforts to the real-life river basin. This program also provided a comprehensive toolkit for simulating various hydrological processes within a watershed. These simulations comprise the determination of surface runoff and flood delineation, both under existing conditions and in managed states, as well as baseflow calculations, water control structure evaluation, and precipitation modeling. Surface runoff is primarily influenced by two sets of factors, namely meteorological elements and the physical properties of the drainage area.

Meteorological elements include crucial variables like precipitation, rainfall intensity, duration, and the spatial distribution of rainfall across the drainage area. However, the physical properties of the drainage area, including land use, soil type, and topographical conditions, also exert a significant impact on surface runoff. These elements of physical

property can be divided into static and dynamic aspects, and these tend to evolve over time. HEC-HMS 4.10 comprises several distinct models, each designed to suit specific hydrological processes with varying input requirements. A common thread across these models is the reliance on time series data, particularly that of hourly rainfall. During the course of the research, the Whisker Box Plot method was used to analyze the maximum rainfall intensity. This approach provides a visually informative representation through bar charts and histograms, allowing for a detailed assessment of data series, including outliers and clustered data points. It simplifies the description of continuous variable distributions by presenting significant statistics such as quartiles, medians, and outliers, including the mean and standard deviation [21]. The quartiles and data distribution used in the rainfall analysis are shown in Figure 4 [22].

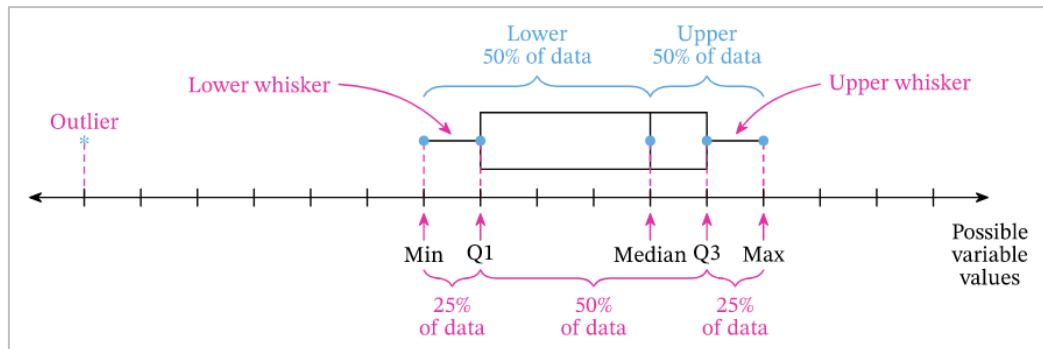


**Figure 4. Whisker and Box Plot Quartile**

Visualizing data using Whisker Box and Plot graphics is a valuable approach for estimating quartiles, medians, and extreme or maximum values [23]. These graphical representations, also known as box plots or box-and-whisker plots, offer insights into various aspects of the data, including central tendencies, distribution characteristics, symmetry extensions, and the identification of outliers [24]. Both box plots and histograms are effective tools for categorizing data and detecting potential outliers, thereby enhancing the analysis process [25]. This method efficiently provides five significant summary statistics for Box-Whisker plots, comprising medians and two quartiles [26].

The second phase of field observations, conducted from May 9 to July 3, 2022, is shown in Figure 5. During this phase, a total of 1295 water level data points were collected, along with an absolute initial pressure of 99.6. To enhance data accuracy, this information was processed using HOBOWare Pro software, ensuring the conversion of water level readings. The results of water level sampling, obtained over approximately five months, are presented in Figure 5.

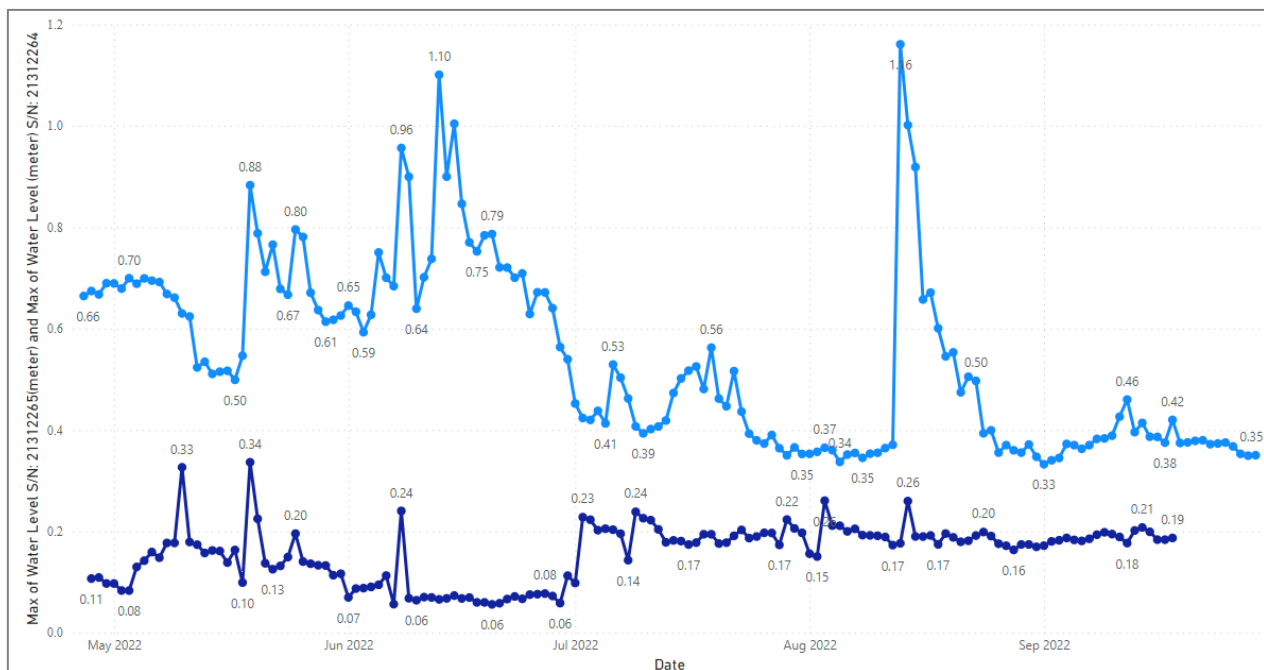


**Figure 5. Water level measurement results from water level sampling in May 2022 until September 2022**

Field observations were conducted at the Ngadirejo (downstream) sampling location, and then a temporary water level graph was plotted starting from May 9 to July 3, 2022. During this period, a total of 1295 water level measurements were collected, while the absolute initial pressure recorded was 99.85 kPa in Ngadirejo (downstream). To capture these

measurements accurately, the HOBOT-S-U20-04 Water Level Data Logger Starter Kit (13") was used. This kit is known for its high-precision water level measurement capabilities, being easily portable, and being cost-effective. It is particularly well-suited for monitoring water levels and temperatures in diverse settings, including wells, rivers, lakes, and freshwater wetlands.

The kit consists of a U20-001-04 HOBOT data logger with a 13-foot range, a BASE-U-4 base station, and five interchangeable couplers, complemented by the BHW-PRO HOBOTware Pro software. The HOBOT Water Level Data Loggers, with a 13-foot range, offer incomparable value and accessibility without complicated vents. During the fieldwork conducted from May 9 to July 2, 2022, a total of 1278 water level measurements were recorded, with an absolute initial pressure reading of 97.453 kPa. To ensure data precision, this information was processed using the HOBOTware Pro software, which facilitated the conversion of data into accurate water level readings. These measurements were crucial for the assessment of water stage and flow discharge.

In an ungauged catchment, the SCS method associates the unit hydrograph lag time with the time concentration ( $t_c$ ) hence:

$$T_{lag} = 0.6 t_c \quad (1)$$

$$t_c = t_{sheet} + t_{shallow} + t_{channel} \quad (2)$$

Using Manning equation, the stream velocity can be estimated as follows:

$$v = \frac{1}{n} R^{2/3} S^{1/2} \quad (3)$$

$$v = \frac{1}{n} \left( \frac{A}{P} \right)^{2/3} S^{1/2} \quad (4)$$

$$v = \frac{1}{0.025} \cdot \left( \frac{31,392 \text{ m}^2}{21,4925 \text{ m}} \right)^{2/3} (0.025)^{1/2} = 8.142 \text{ m/s}$$

To calculate the 't' channel, use the following equation, where 'L' represents the river length, and 'V' represents the stream velocity.

$$t_{channel} = \frac{L}{V} \quad (5)$$

The definition of Peak Discharge (Q) is simply calculated by dividing the direct runoff by the total runoff volume, where P is the cumulative precipitation for an event in mm units, CN is the curve number, S is the potential maximum retention in mm, is the initial proportional abstraction in mm, and  $\lambda$  is the initial abstraction coefficient (dimensionless) [27]. The general form of the rational formula used in this research is obtained by Equation 6 [27].

$$Q = 0.2778 \cdot C \cdot I \cdot A \quad (6)$$

Therefore, Q, C, I, and A is peak flow or discharge, runoff coefficient, maximum rainfall intensity, and the catchment area, respectively.

The studied basin covers an area of 91.526 km<sup>2</sup>, with a river length and width of 40.37 km and 2.285 km, respectively. It exhibited a time concentration in the channel lasting 4948.24 seconds, along with a 24-minute time lag. In the HEC HMS 4.10 Model, the initial step constituted the establishment of basin models, which include sub-basins. Subsequent to sub-basin delineation, the initial parameters are defined, and these comprise the loss method, direct runoff, canopy, surface, and baseflow. For predicting runoff, the SCS-CN method, which relies on three critical parameters, namely Initial Abstraction ( $I_a$ ), Curve Number (CN), and an impervious area ranging from 0 to 2%, was used.

To determine direct runoff, an SCS Unit Hydrograph is used, incorporating parameters like lag time and concentration time. These calculations are based on stream velocity data, determined through the Manning equation. In the context of runoff modeling, various components and parameters play a critical role, directly impacting the modeling process as they are compared with model simulations. The primary focus of runoff modeling is to simulate the transformation of rainfall into discharge, with specific attention given to calculating peak flow and direct runoff within the watershed. Table 1 presents data related to the parameters of the basin models used in HEC HMS.

**Table 1. Parameters Data Basin Models in HEC HMS**

Scenarios	Basin models	Scenarios
Loss method	SCS-CN	Loss method
Transform	SCS Unit Hydrograph	Transform
Routing	Lag	Routing



The function of the data control specifications is to organize the operational period and effectively manage the duration of runoff rainfall modeling. Within this simulation, a Specified Hyetograph was used as the selected precipitation model. This simulation relies on a rating curve, with primary parameters including the excess rainfall area, daily precipitation excluding baseflow, and peak discharge.

## 2.1. Research Area

The observation and fieldwork approach comprised a two-point sampling method. This choice was made due to the Brantas River's distinct characteristics, characterized by a variety of natural channels that result in consistently elevated water discharge levels throughout the year. The specific selection of this area is based on its classification as an ungauged catchment, which underscores its significance in terms of conservation. The Lanang River Basin, located within this catchment, covers an area of 91.526 km<sup>2</sup>, with a length and width of 40.37 km and 2.285 km, respectively. A more detailed overview of its characteristics is shown in Table 2.

**Table 2. Physical Catchment Area of Study located**

Typical	Symbol	Unit	
Drainage Area	A	km <sup>2</sup>	91.526
Length	L	Km	40.083
Slope	S	Routing	0.002

The research area is located in the Lanang River catchment, which is part of the Brantas River in Kediri, East Java, Indonesia, as shown in Figure 6.

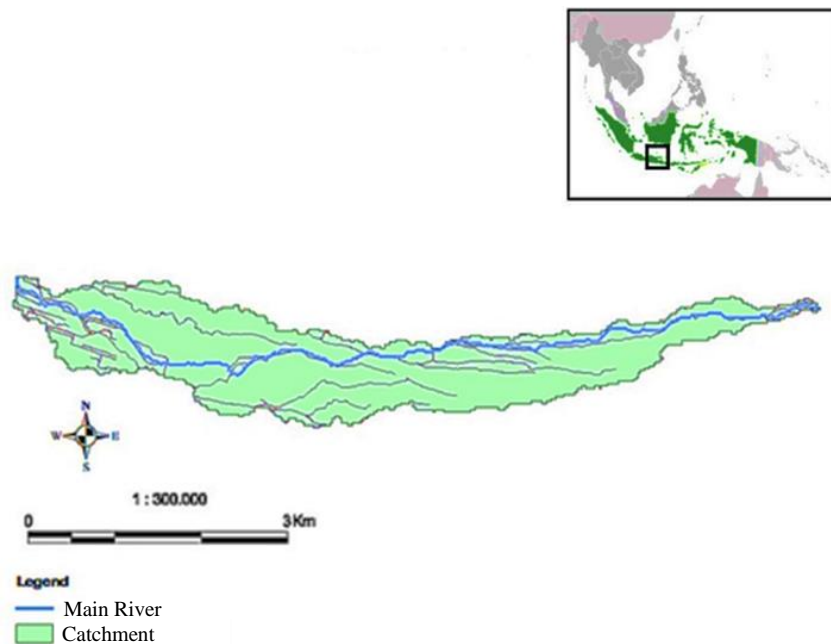


**Figure 6. The Catchment Area of Study is located in Lanang River, Kediri, East Java Indonesia**

## 3. Results and Discussion

### 3.1. Analysis Whisker and Box Plot

In this research, the Whisker Box method was employed, which was selected because it effectively illustrates varying data quantities with detailed bar charts and histograms, which provide a clear visual representation. This method not only enables the identification of outliers and the visualization of clustered data points but also simplifies the expression of data distribution for continuous variables. It offers insights into quartiles, medians, and outliers, as well as mean and standard deviation [18]. Figure 7 is a graphical representation of the highest rainfall obtained in 2019 using the whisker box plot, where the maximum rainfall occurred in 2021 at a depth of 140 mm.

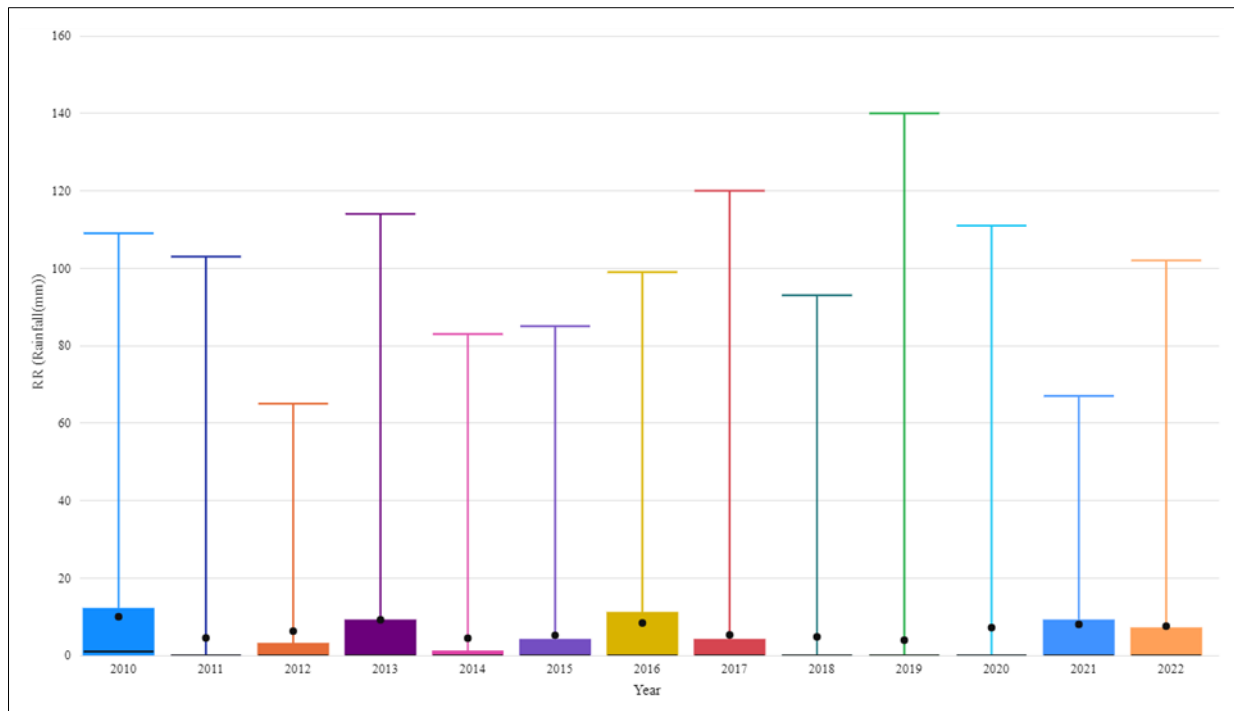


Figure 7. Maximum Rainfall Intensity in Whisker and Box Plot

### 3.2. Rating Curve Analysis

In hydrology, a rating curve is a fundamental tool that presents the relationship between discharge and water level at a specific point along a watercourse. These curves are typically constructed at measuring stations positioned across the flow channel and are created using data from two automatic water level recorders (AWLL). According to Kennedy (1984), the rating curve graphically shows discharge on the x-axis and water level (stage) on the y-axis. The main purpose of employing automatic water level loggers within the river channel is to obtain water level measurements, which are vital for determining runoff flow and, ultimately, finding peak flow within the Lanang watershed. The rating curve essentially serves as an expression of the connection between water level and discharge at a particular location along the river cross-section [28]. It involves the analysis of discharge measurements in correlation with the elevation of the water table, resulting in the derivation of a regression curve that describes the relationship between discharge and water table elevation. This rating curve analysis extends to the downstream limit condition, including a comprehensive assessment of the discharge measurement results in conjunction with water table elevation.

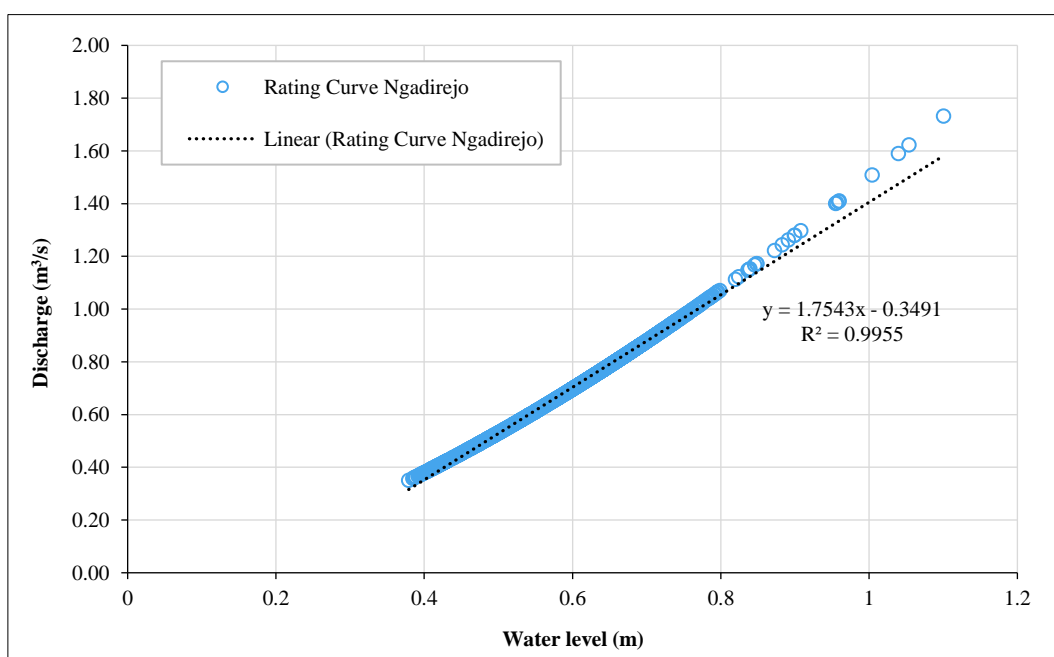
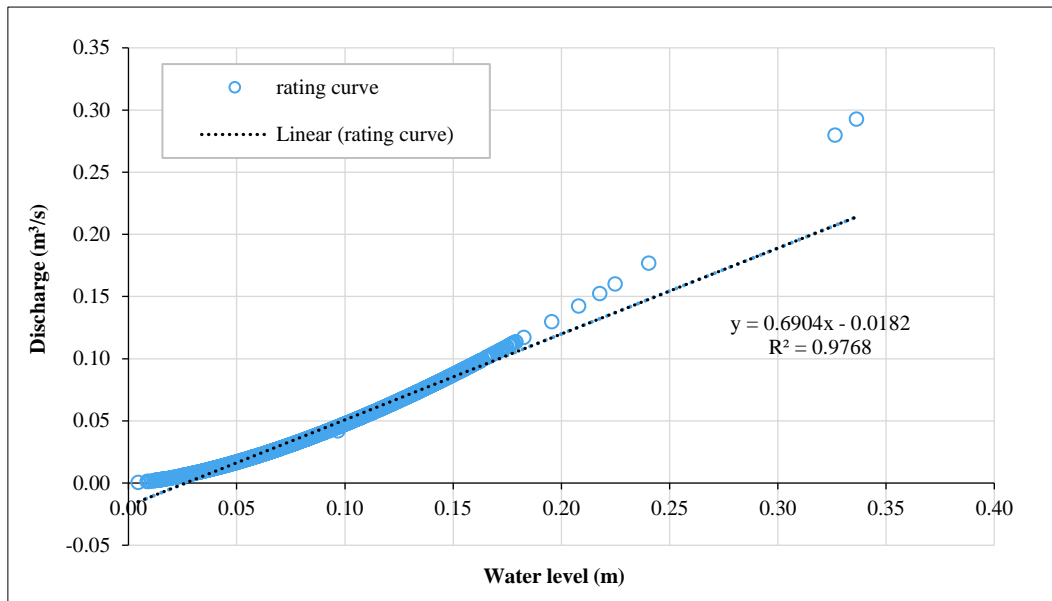


Figure 8. Rating curve analysis for downstream Ngadirejo

Figure 9 shows the rating curve obtained at the downstream automatic water level logger in Ngadirejo. The equation associated with this curve exhibits an impressive R-square value of 0.9955, as well as the rating curve at Pandantoyo AWLL placement.



**Figure 9. Rating curve analysis for upstream Pandantoyo**

This research examined the analysis of time-series data from 2022 using rainfall-runoff modeling and compared the results with field measurements from April 28, 2022, to June 30, 2022. The data included rainfall observations from rain gauges paired with discharge measurements. The data for HEC-HMS 4.10 and the open-channel Manning method equation were used to predict hydraulic conductivity, porosity, lag, and stream velocity ( $n = 0.025$ ). The calculations, based on the S formulation in the SI system, yielded an S value of 133.78 mm [4]. This study employed the CN method, derived from SCS-CN, with the initial abstraction ( $I_a$ ) determined using an  $I_a/S$  ratio set at 0.2, which resulted in a calculated value of  $I_a = \lambda S = 0.2 \times 133.78 = 26.756$ . Through analysis in Microsoft Excel and hydrological soil group (HSG) classification, it was found that the composite CN was 65.50. The study encompassed three types of simulations, namely one basin, multi-basins, and typical basins. The Lamong River catchment area was selected as a typical catchment for simulation and comparison with the Lanang River catchment, owing to its similar shape, belonging to the Bengawan Solo River system, and sharing criteria such as land use, soil conditions, and parameters used in HEC HMS [29–31].

### 3.3. The Scenario for Comparison between Time Series Modeling and Fieldwork Data

Numeric modeling was conducted using three different models, including (a) one sub-basin, (b) a multi-basin, and (c) a typical catchment. For the single sub-basin simulation model, the initial optimization trial utilized data collected from an automatic water level logger located at Pandantoyo. This trial focused on sensitivity parameter values related to SCS CN-CN and lag time parameters, with the initial CN value set at 65.56, using minimum and maximum values of 43 and 99. Additionally, simulation models in a single sub-basin were examined using data from an automatic water level logger positioned at Pandantoyo for the first optimization trial. This trial involved sensitivity parameter analysis for both SCS Curve Number-Curve Number and SCS Curve Number-Lag Time parameters, maintaining an initial CN value of 65.56, a minimum of 43, and a maximum of 99. Figure 9 shows a graph of the single sub-basin, depicting data on precipitation, excess rainfall, and outflow. This data was obtained from running simulations using the HEC HMS 4.10 application. Numeric modeling was conducted in multibasin for trial optimization of SCS Curve Number- Curve Number.

### 3.4. Sensitivity Analysis Parameters using SCS Curve Number

Calibration plays a crucial role in ensuring that our model closely resembles reality; hence, paired data from upstream and downstream data loggers within a multi-basin model was used in this research. To organize the catchment, it was divided into five sub-basins, corresponding to the various branches of the river and their convergence into the main river. This experimentation involved three types of simulations: one basin, multi-basins, and typical rectangular basins. The Lamong River catchment area was selected as a representative rectangular catchment for comparison purposes because it shared similar characteristics with the study catchment, including land use, soil conditions, and parameters in HEC HMS. The calibration process involved three optimization scenarios, each involving two varying parameters,



namely the SCS Curve Number parameter with Curve Number, the SCS Curve Number with lag time, and the SCS Curve Number with Initial Abstraction. These scenarios were applied to both a single sub-basin and a multi-basin model, consisting of five sub-basins.

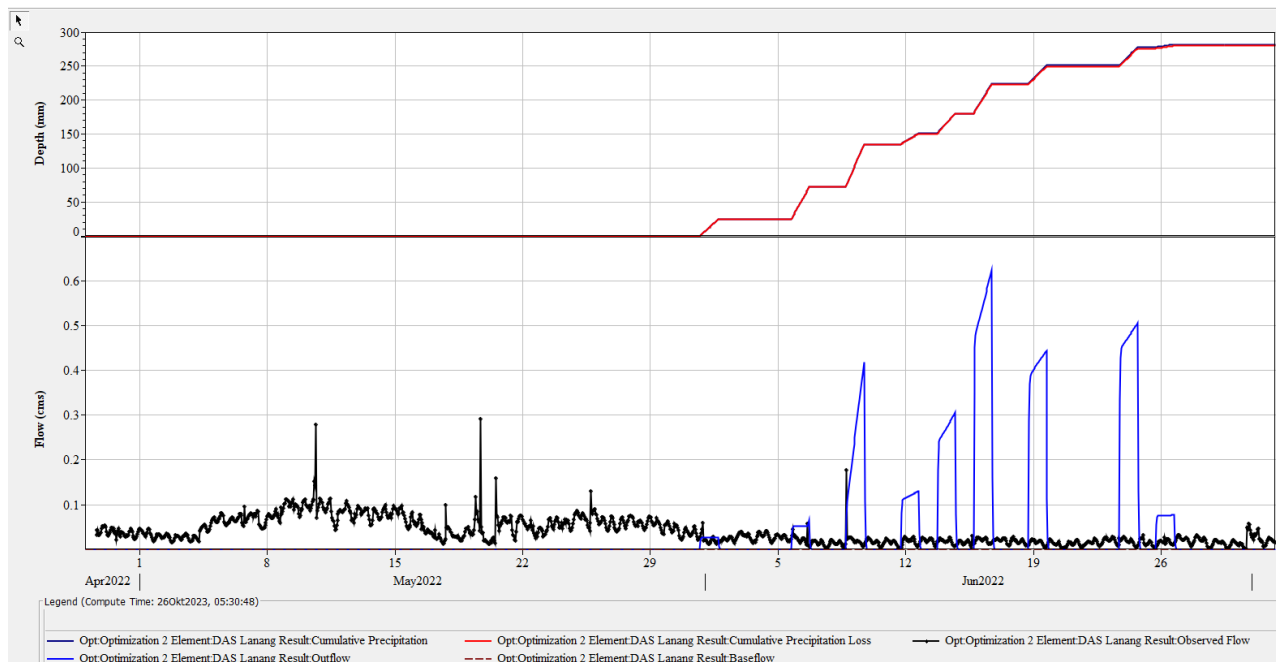


Figure 10. Simulation one basin, upstream paired data

The selection of the Lamong River basin for comparison was due to its ungauged catchment and logistical constraints, which prevented the installation of automatic water level recorders. In modeling the Lanang watershed sub-basin, a basin model manager was used with a Southern WGS 84 UTM 49S coordinate system, while an automatic water level logger was used to populate the paired data. The water level data were tabulated in a logger table, categorized into upstream and downstream conditions. In summary, the initial modeling results indicated a significant disparity between the observations. The simulation yielded a peak discharge of 89.7 m<sup>3</sup>/s, while the observed peak discharge was only 1.7 m<sup>3</sup>/s, as depicted in Figure 10. In hydrology, hydrological model parameters were examined to suit specific watersheds through the calibration and validation of observed river flows. However, predicting river flow in ungauged catchment areas, where discharge data is not available, remains a significant challenge [32].

Sensitivity analysis (SA) plays a crucial role in hydrological modeling by helping identify which parameters influence the model and providing insights into the relationships between various processes within the system [33]. Furthermore, the validity of the CN model is determined through observations and its correlation with CNs, along with direct field measurements [34]. The optimization scenario involved two distinct parameters, as cited in Nazif et al. [35]. In the third optimization case, two varied parameters were considered, namely lag time and SCS-CN with  $I_a$ . To calibrate the model in this study, various scenarios were employed, including one sub-basin, a multi-basin (comprising five sub-basins), and a comparison with other watersheds sharing a similar rectangular watershed shape to Lanang. Therefore, the Lamong catchment was selected due to its ability to ungauged and automate water level recorders (AWLL) for unavailable measurement. Calibration is crucial to ensuring the simulated model closely approximates real-world conditions. For digitizing the Lanang watershed sub-basin, a basin model manager with a Southern WGS 84 UTM 49S coordinate system was used. The data logger was placed at Pandantoyo (upstream), a river that approaches the river mouth near the coast.

### 3.5. Modify Runoff Coefficient

Effective rainfall, which represents the portion of rain contributing to river flow, is a critical factor in hydrology [36]. It significantly influences the calculation of the runoff coefficient [36]. While the standard analysis of effective rainfall typically considers a 25-year return period [37], this research focuses on a ten-year return period. The rational method for calculating peak flow relies on several parameters, including rainfall intensity, runoff coefficient, and catchment area [37, 38]. However, it is essential to emphasize that the determination of peak flow in a catchment extends beyond the use of rational methods and also considers additional factors such as rainfall patterns and time of concentration [39]. Previous research has identified correlations between the curve number (CN), runoff coefficient, and rainfall. The volume includes observed and model runoff [40], obtained from rainfall-paired data with respect to flow hydrographs

[40]. In contrast, the curve number method was used to obtain the runoff model [16]. These correlations comprise various aspects, including maximum rainfall intensity and excess rainfall calculated using the Mononobe method. The visual representation of this correlation from 2010 to 2022 is shown in Figure 11.

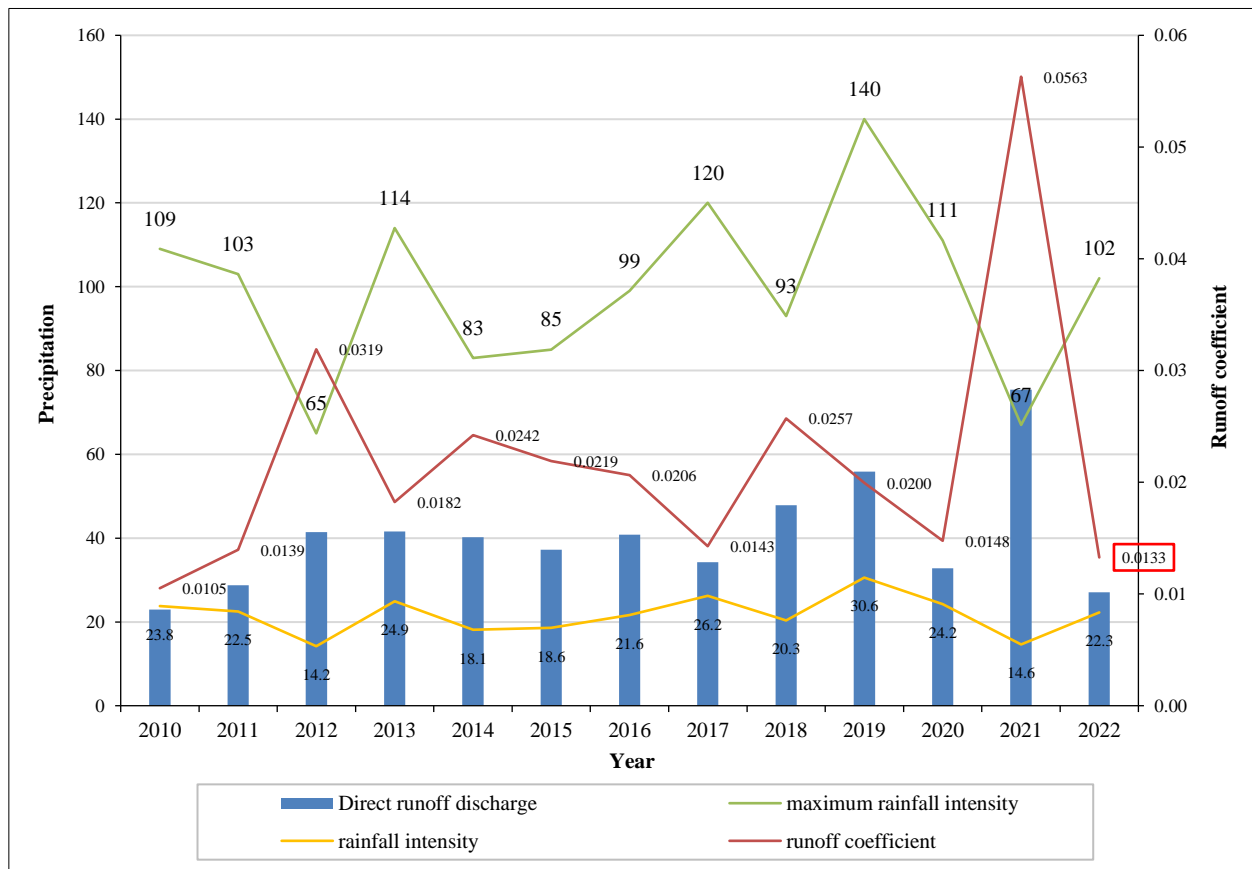


**Figure 11. Maximum Rainfall Intensity Relationship, Average Rainfall Intensity Mononobe Method, Runoff Coefficient in the year 2010 to 2022**

The runoff coefficient, which is calculated based on peak flow ( $Q$ ) derived from in-situ water level measurements, exhibits a significant correlation with increasing maximum rainfall intensity. Summarizing the results of simulations conducted in a single sub-basin within the Lanang watershed, a significant disparity was observed between the initial modeling results and the actual field measurements. The model predicted a peak discharge of  $0.1 \text{ m}^3/\text{s}$ , while the field measurements recorded a higher value of  $0.3 \text{ m}^3/\text{s}$ . Therefore, it is evident that further refinement and iteration of the model are necessary to correlate with the observed field results.

## 4. Conclusion

In conclusion, the primary objectives of this research were to refine the runoff coefficient using the rational method approach and to compare the results of peak discharge obtained through numerical rainfall modeling, focusing on specific key parameters. The motivation for conducting this research in the Lanang River Basin, an ungauged catchment, was due to a lack of data and susceptibility to discharge-related issues. However, the findings revealed that the runoff coefficient increased in conjunction with discharge. When analyzing peak discharge values for maximum rainfall intensity, the following results were obtained, observational data yielded peak discharge values of  $405.7 \text{ m}^3/\text{s}$ ,  $304.3 \text{ m}^3/\text{s}$ , and  $25 \text{ m}^3/\text{s}$ . Direct runoff estimations for C coefficients of 0.60, 0.45, and 0.0133 correspondingly produced peak discharge values in 2022.

## 5. Declarations

### 5.1. Author Contributions

Conceptualization, M.A.M. and M.K.; methodology, M.A.M. and M.K.; software, M.K.; validation, D.I., M.A.M. and M.K.; formal analysis, M.A.M.; investigation, M.K.; resources, M.A.M. and M.K.; data curation, M.A.M.; writing—original draft preparation, M.K.; writing—review and editing, D.I. and M.A.M.; visualization, D.I. and M.A.M.; supervision, D.I. and M.A.M.; project administration, M.K.; funding acquisition, M.K. All authors have read and agreed to the published version of the manuscript.

## 5.2. Data Availability Statement

The data presented in this study are available in the article.

## 5.3. Funding

The authors received no financial support for the research, authorship, and/or publication of this article.

## 5.4. Institutional Review Board Statement

Not applicable.

## 5.5. Informed Consent Statement

Not applicable.

## 5.6. Declaration of Competing Interest

The authors declare that there is no conflict of interests regarding the publication of this manuscript. In addition, the ethical issues, including plagiarism, informed consent, misconduct, data fabrication and/or falsification, double publication and/or submission, and redundancies have been completely observed by the authors.

## 6. References

- [1] Lee, K. K. F., Ling, L., & Yusop, Z. (2023). The Revised Curve Number Rainfall–Runoff Methodology for an Improved Runoff Prediction. *Water (Switzerland)*, 15(3), 491. doi:10.3390/w15030491.
- [2] Hayes, D. C., & Young, R. L. (2006). Comparison of peak discharge and runoff characteristic estimates from the rational method to field observations for small basins in central Virginia. *Scientific Investigations Report*. doi:10.3133/sir20055254.
- [3] Wainwright, J., & Parsons, A. J. (2002). The effect of temporal variations in rainfall on scale dependency in runoff coefficients. *Water Resources Research*, 38(12), 7-17–10. doi:10.1029/2000wr000188.
- [4] Singh, J., Altinakar, M. S., & Ding, Y. (2015). Numerical Modeling of Rainfall-Generated Overland Flow Using Nonlinear Shallow-Water Equations. *Journal of Hydrologic Engineering*, 20(8). doi:10.1061/(asce)he.1943-5584.0001124.
- [5] Pilgrim, W., Eaton, P., & Trip, L. (2001). The need for integrated linkages and long-term monitoring of mercury in Canada. *Environmental Monitoring and Assessment*, 67(1–2), 57–68. doi:10.1023/A:1006431617093.
- [6] El Bouanani, L., Baba, K., Ardouz, G., & Latifi, F. E. (2022). Parametric Study of a Soil Erosion Control Technique: Concrete Lozenges Channels. *Civil Engineering Journal*, 8(9), 1879–1889. doi:10.28991/CEJ-2022-08-09-09.
- [7] Hosseiny, H., Crimmins, M., Smith, V. B., & Kremer, P. (2020). A generalized automated framework for urban runoff modeling and its application at a citywide landscape. *Water (Switzerland)*, 12(2), 357. doi:10.3390/w12020357.
- [8] Pappas, E. A., Smith, D. R., Huang, C., Shuster, W. D., & Bonta, J. V. (2008). Impervious surface impacts to runoff and sediment discharge under laboratory rainfall simulation. *Catena*, 72(1), 146–152. doi:10.1016/j.catena.2007.05.001.
- [9] Pennington, S. L., & Webster-Brown, J. G. (2008). Stormwater runoff quality from copper roofing, Auckland, New Zealand. *New Zealand Journal of Marine and Freshwater Research*, 42(1), 99–108. doi:10.1080/00288330809509940.
- [10] Salami, A. W., Bilewu, S. O., Ibitoye, A. B., & Ayanshola, A. M. (2017). Runoff hydrographs using Snyder and SCS synthetic unit hydrograph methods: A case study of selected rivers in south west Nigeria. *Journal of Ecological Engineering*, 18(1), 25–34. doi:10.12911/22998993/66258.
- [11] Kim, N. W., Shin, M.-J., & Lee, J. E. (2016). Application of runoff coefficient and rainfall-intensity-ratio to analyze the relationship between storm patterns and flood responses, *Hydrology and Earth System Sciences (Preprint)*. doi:10.5194/hess-2016-194.
- [12] Nagy, E. D., Torma, P., & Bene, K. (2016). Comparing Methods for Computing the Time of Concentration in a Medium-Sized Hungarian Catchment. *Slovak Journal of Civil Engineering*, 24(4), 8–14. doi:10.1515/sjce-2016-0017.
- [13] Dhakal, N., Fang, X., Cleveland, T. G., Thompson, D. B., Asquith, W. H., & Marzen, L. J. (2012). Estimation of Volumetric Runoff Coefficients for Texas Watersheds Using Land-Use and Rainfall-Runoff Data. *Journal of Irrigation and Drainage Engineering*, 138(1), 43–54. doi:10.1061/(asce)ir.1943-4774.0000368.
- [14] Pool, S., & Seibert, J. (2021). Gauging ungauged catchments – Active learning for the timing of point discharge observations in combination with continuous water level measurements. *Journal of Hydrology*, 598, 126448. doi:10.1016/j.jhydrol.2021.126448.
- [15] Nossent, J., & Bauwens, W. (2012). Multi-variable sensitivity and identifiability analysis for a complex environmental model in view of integrated water quantity and water quality modeling. *Water Science and Technology*, 65(3), 539–549. doi:10.2166/wst.2012.884.

- [16] Chin, D. A. (2023). Discussion of “NRCS Curve Number Method: Comparison of Methods for Estimating the Curve Number from Rainfall-Runoff Data.” *Journal of Hydrologic Engineering*, 28(8). doi:10.1061/jhyeff.heeng-5904.
- [17] Agashua, L. O., Oluyemi-Ayibiowu, B. D., Ihimekpen, N. I., & Igibah, E. C. (2022). Modeling the semivariogram of climatic scenario around rivers by using stream network mapping and hydrological indicator. *Journal of Human, Earth, and Future*, 3(1), 17-31. doi:10.28991/HEF-2022-03-01-02.
- [18] Kencanawati, M., Anwar, N., & Maulana, M. A. (2021). Modification of basic hydrology formulation based on an approach of the rational method at field measurement. *IOP Conference Series: Earth and Environmental Science*, 930(1), 12051. doi:10.1088/1755-1315/930/1/012051.
- [19] Kotu, V., & Deshpande, B. (2019). Time Series Forecasting. *Data Science*, 395–445, Morgan Kaufmann, Burlington, United States. doi:10.1016/b978-0-12-814761-0.00012-5.
- [20] Kirmani, S. N. U. A., Montgomery, D. C., Runger, G. C., & Hubele, N. F. (2000). *Engineering Statistics*. The American Statistician, 54(3), 226. doi:10.2307/2685597.
- [21] Forthofer, R. N., Lee, E. S., & Hernandez, M. (2007). *Linear Regression*. Biostatistics, 349–386, Academic Press, Cambridge, United States. doi:10.1016/b978-0-12-369492-8.50018-2.
- [22] Meloun, M., & Militký, J. (2011). Statistical analysis of univariate data. *Statistical Data Analysis*, 73–150. doi:10.1533/9780857097200.73.
- [23] Ramachandran, K. M., & Tsokos, C. P. (2015). *Descriptive Statistics*. Mathematical Statistics with Applications in R, 1–52, Academic Press, Cambridge, United States. doi:10.1016/b978-0-12-417113-8.00001-1.
- [24] Kennedy, E. J. (1984). Discharge ratings at gaging stations. *Techniques of Water-Resources Investigations* 03-A10, U.S. Geological Survey, Reston, United States. doi:10.3133/twri03a10.
- [25] Schumann, A. H. (1999). *Hydrometry—Principles and Practices*, Second edition; R.W. Herschy (Ed.); John Wiley & Sons, Chichester, 1999 Hardcover, VI+376pp., Price £75.00., ISBN 0-471-97350-5. *Journal of Hydrology*, 222(1–4), 191–192. doi:10.1016/s0022-1694(99)00091-8.
- [26] Walega, A., Amatya, D. M., Caldwell, P., Marion, D., & Panda, S. (2020). Assessment of storm direct runoff and peak flow rates using improved SCS-CN models for selected forested watersheds in the Southeastern United States. *Journal of Hydrology: Regional Studies*, 27(1–4), 191–192. doi:10.1016/j.ejrh.2019.100645.
- [27] Gebresellassie Zelelew, D. (2017). Spatial mapping and testing the applicability of the curve number method for ungauged catchments in Northern Ethiopia. *International Soil and Water Conservation Research*, 5(4), 293–301. doi:10.1016/j.iswcr.2017.06.003.
- [28] Wang, S., & Wang, H. (2018). Extending the Rational Method for assessing and developing sustainable urban drainage systems. *Water Research*, 144, 112–125. doi:10.1016/j.watres.2018.07.022.
- [29] Mann, R., & Gupta, A. (2022). Temporal trends of rainfall and temperature over two sub-divisions of Western Ghats. *HighTech and Innovation Journal*, 3, 28-42. doi:10.28991/HIJ-SP2022-03-03.
- [30] Vonnisa, M., Shimomai, T., Hashiguchi, H., & Marzuki, M. (2022). Retrieval of vertical structure of raindrop size distribution from equatorial atmosphere radar and boundary layer radar. *Emerging Science Journal*, 6(3), 448-459. doi:10.28991/ESJ-2022-06-03-02.
- [31] Amatya, D. M., Walega, A., Callahan, T. J., Morrison, A., Vulava, V., Hitchcock, D. R., Williams, T. M., & Epps, T. (2022). Storm event analysis of four forested catchments on the Atlantic coastal plain using a modified SCS-CN rainfall-runoff model. *Journal of Hydrology*, 608, 127772. doi:10.1016/j.jhydrol.2022.127772.
- [32] Fanta, S. S., & Sime, C. H. (2022). Performance assessment of SWAT and HEC-HMS model for runoff simulation of Toba watershed, Ethiopia. *Sustainable Water Resources Management*, 8(1). doi:10.1007/s40899-021-00596-8.
- [33] Hadiani, R. R. (2020). Analysis of Drainage Capacity as a Flood Control Effects in Laweyan Sub-District. *International Journal of GEOMATE*, 19(74), 222–228. doi:10.21660/2020.74.24829.
- [34] Baiamonte, G. (2020). A rational runoff coefficient for a revisited rational formula. *Hydrological Sciences Journal*, 65(1), 112–126. doi:10.1080/02626667.2019.1682150.
- [35] Chin, D. A. (2019). Estimating Peak Runoff Rates Using the Rational Method. *Journal of Irrigation and Drainage Engineering*, 145(6). doi:10.1061/(asce)ir.1943-4774.0001387.
- [36] Nazif, S., Soleimani, P., & Eslamian, S. (2022). Dynamic Curve Numbers. *Flood Handbook*, 357–384. doi:10.1201/9781003262640-22.

- [37] Selbig, W. R., Loheide, S. P., Shuster, W., Scharenbroch, B. C., Coville, R. C., Kruegler, J., Avery, W., Haefner, R., & Nowak, D. (2022). Quantifying the stormwater runoff volume reduction benefits of urban street tree canopy. *Science of the Total Environment*, 806, 151296. doi:10.1016/j.scitotenv.2021.151296.
- [38] Ben Khélifa, W., & Mosbahi, M. (2022). Modeling of rainfall-runoff process using HEC-HMS model for an urban ungauged watershed in Tunisia. *Modeling Earth Systems and Environment*, 8(2), 1749–1758. doi:10.1007/s40808-021-01177-6.
- [39] Prokešová, R., Horáčková, Š., & Snopková, Z. (2022). Surface runoff response to long-term land use changes: Spatial rearrangement of runoff-generating areas reveals a shift in flash flood drivers. *Science of the Total Environment*, 815, 151591. doi:10.1016/j.scitotenv.2021.151591.
- [40] Beven, K. (2012). Predicting Hydrographs Using Models Based on Data. In *Rainfall-Runoff Modelling*. John Wiley & Sons, Hoboken, United States. doi:10.1002/9781119951001.ch4.